Journal of Petroleum Exploration and Production Technology (2019) 9:1443–1455
https://doi.org/10.1007/s13202-018-0539-z

ORIGINAL PAPER - PRODUCTION ENGINEERING

Laboratory investigation of asphaltene-induced formation damage

I. A. Struchkov[1] · M. K. Rogachev[1] · E. S. Kalinin[2] · P. V. Roschin[3]

Received: 21 June 2018 / Accepted: 20 August 2018 / Published online: 24 August 2018

Abstract

The purpose of this study is to evaluate the degree of formation damage caused by asphaltene deposition in the pore throats in case of oilfield operation. Many wells in the Samara region oilfields are operated under high reservoir drawdown, with downhole pressure lower than the bubble point. Such wells' operating conditions lead to a change in oil composition (light components are extracted from oil while asphaltenes are precipitated and deposited) in the near wellbore, and the productivity of the wells declines due to asphaltene deposition. The study procedure presented in the paper included the following methods: high-pressure microscopy with grain size analysis (the visual method), the near infrared light scattering method and the gravimetric method to measure asphaltenes onset pressure in oil. Formation damage was measured by the filtration method. Asphaltene concentration in oil after filtration was measured by the photocolorimetric analysis. Microcomputed tomography of the core sample was provided to visualize formation damage. In addition, fluid flow in the pore space was simulated before and after asphaltene deposition using a dynamic simulator. In the paper, reservoir oil of one of the Russian oilfields was investigated. The main results of this paper are the following: asphaltene onset pressure in oil at the reservoir temperature (48 °C) was measured as equal to 6.8 MPa which is slightly higher than the bubble-point (6.5 MPa). Oil was flowed through the core sample of the field at three different specific backpressures (at constant flow rate) and formation damage was estimated. The studies have shown that decrease in permeability of the core is caused by asphaltene deposition in the pore space. In this case, a decrease in the amount of asphaltenes in oil emerging from the core sample is observed which was proved by the spectrophotometric analysis. Via microcomputed tomography, a 3D model of the rock matrix and the pore space of the initial and damaged core sample was constructed and a decrease in porosity after formation damage was estimated. Based on the obtained 3D model of the core, computer simulation of fluid flow (in a dynamic simulator) in the initial and damaged core was performed, and the flow parameters (velocity and streamlines) were calculated. The proposed methodology including a set of physical methods to study a core before and after formation damage combined with fluid flow simulation enables predicting potential complications under the field operation.

Keywords Formation damage · Asphaltenes precipitation · Onset pressure · Reservoir oil · Permeability reduction

Introduction

During field production at natural depletion, under injection natural gas or CO_2, thermobaric conditions of oil in situ alter as well as its composition. As a result, solubility of oil according to asphaltene changes, and they precipitate in oil (Hirschberg et al. 1984; Leontaritis 1989; Burke et al. 1990). Some of them may deposit in the near-wellbore area thus leading to formation damage and reducing oil production (Sharma et al. 1985; de Pedroza et al. 1996; Minssieux 1997; Ali and Islam 1998; Shedid 2001). Such phenomenon can be observed even though asphaltenes in oil until that time were in equilibrium state.

In 1972, in Western Texas, injection of CO_2 was first tested in the Perm oil-and-gas-bearing basin (Kokal and Al-Kaabi 2010). The discovery of large reserves of CO_2 led to further growth in the use of gas EOR in the USA. The maximum growth in the use of this technology in the USA was achieved in the late 1980s despite low oil prices. In Russia, pilot projects of this technology started in the

✉ I. A. Struchkov
StruchkovIA@gmail.com

[1] "Development and Exploitation of Oil and Gas Fields" Department, Saint-Petersburg Mining University, 21st Line, Saint Petersburg 199106, Russia

[2] LLC SamaraNIPIneft, Samara, Russia

[3] LLC SNK, Saint Petersburg, Russia

1980s. However, this method was not extensively implemented in the industry.

It should be noted that JSC RITEK resumed field trials of the carbon dioxide flooding technology as an EOR method (Volkov et al. 2017) at heavy oil reservoirs in Samara (Russia). The authors (Struchkov et al. 2016) analyzed about 150 oilfields in the Samara region. They noted that downhole pressure of many wells in some fields dropped below the bubble point. Some studies (Novosad and Costain 1990) show that oils with similar characteristics under such conditions tend to precipitate asphaltenes when interacting with carbon dioxide. Therefore, there is much concern about challenge caused by asphaltene deposition in these fields for the operator companies.

J. B. Boussingault was the first to discover bitumen (asphaltenes) in Eastern France in 1837 and gave them this name. According to modern concepts, asphaltenes are the heaviest and polar oil components and they contain metals in the structure. They are soluble in aromatic hydrocarbons and insoluble in *n*-alkanes (Speight et al. 1984; Khalil et al. 1997). In oil, they are represented by floccules or aggregates of solid asphaltene particles with resins adsorbed onto their surface that prevent their further aggregation (Nellensteyn 1924; Bunger and Li 1981).

Asphaltene aggregation in oil is a very complex process and in spite of the fact that this challenge is found out many years ago, it remains poorly studied currently. Before assessment of complications in the field, it is necessary to evaluate influence of many factors on asphaltene aggregation in oil. Authors of the paper (Mozaffari et al. 2017) have investigated solutions of asphaltenes and bitumen in various solvents with aging. It has been shown that over time the viscosity of solutions decreases that is due to asphaltene aggregation and reduction of effective volume fractions of bitumen and asphaltenes in solution. Viscosity of solutions on the basis of aromatic hydrocarbons does not change essentially, and the highest rate of asphaltene precipitation is observed in solvents based on saturated hydrocarbons that confirms poor solubility of asphaltenes in them.

Authors of the paper (Mozaffari et al. 2015) have investigated rheological properties of solutions of asphaltenes and bitumen in heptol (a mixture of heptane and toluene at the volume ratio of 80/20) in nanochannels. Authors proved that with increase in concentration of bitumen solution, solution begins to show more non-Newtonian behavior and it can be better described by a non-Newtonian Bingham Plastic model. The authors observed the blocking of nanochannels at achievement of a certain concentration of asphaltenes in solution. It is associated with the presence in solution of asphaltene aggregates similar in size to nanochannels.

The aromatic nature of asphaltenes largely determines the chemical technologies used to control their deposition, for example, the efficiency of deposits' inhibition is determined by the content of aromatic components in an inhibitor.

Another effective method used to prevent asphaltene deposition is control wells operating conditions, when downhole pressure maintains above the bubble point. To successfully prevent asphaltene deposition, it is necessary to investigate their interaction with other oil components, porous media and inhibitors. Many modern research methods, such as dynamic and static methods used to study conditions for asphaltene deposition in oil, are aimed to solving this challenge. The most popular methods to study asphaltene deposition are light scattering, gravimetric techniques (static), and filtration (dynamic) which were used in this paper. Other research methods are also known, such as fluorescence spectroscopy, conductive measurement, acoustic resonance, etc.

There are several approaches to assess colloidal state of asphaltenes in oil. According to the colloidal model, asphaltenes in oil are in the equilibrium state at the ratio of resin to asphaltenes larger than 1.25. However, this approach is not verified for all oils.

Yen introduced the colloidal instability index (CII) term which allows to estimate more precisely the possibility of asphaltene precipitation in oil:

$$\mathrm{CII} = \frac{(\mathrm{Saturates} + \mathrm{Asphaltenes})}{(\mathrm{Aromatics} + \mathrm{Resins})}. \quad (1)$$

According to his model, if the index is less than 0.7, asphaltenes remain stable in oil. If the index exceeds 0.9, then there is high probability of asphaltene precipitation in oil.

Equation 1 was proposed by Yen as the express estimation method of asphaltene precipitation, without carrying out additional special studies. All the express techniques and equations anyway base on a limited number of oil samples of a certain origin. This equation has been mentioned by authors of the paper as an example which was confirmed in this study. Oil of the Russian fields also complies with the colloidal instability index calculated on the basis of SARA analysis. This equation shows that oil prone to asphaltene deposition, undersaturated with resins and aromatics which are stabilizers of asphaltenes. Thus, the change in thermobaric conditions leads to faster desorption of resins from the asphaltene surface and further aggregation of asphaltenes.

Mansoori and Leontaritis have proposed a model according to which the amount of adsorbed resins onto the asphaltene surface is a function of their concentration in oil. When thermodynamic equilibrium of resins in oil is disturbed, they are desorbed from the surface of asphaltenes which causes asphaltenes to aggregate and precipitate.

One of the worst options happens when asphaltenes are deposited in a reservoir. The challenge in modeling

formation damage is that the pore space in a reservoir has a very complex structure. Previously, simplified models (Gruesbeck and Collins 1982) were obtained with the pore space represented by parallel pathways. That model included empirical correlations between permeability reduction and concentration of solids in a fluid. Later, another model was created (Sahimi et al. 2000) that took into account adsorption of asphaltenes on the surface of pore throats and their plugging.

One of the most responsible and accessible methods is the one proposed by Leontaritis who presented in 1998 a simplified analytical model for formation damage in single-phase state. He proposed the following assumptions: reservoir pressure and the asphaltene onset pressure remain constant; asphaltene precipitation occurs in the near-wellbore area, uninvaded area is not affected by this phenomenon, and the decrease in permeability occurs due to plugging pore throats by asphaltenes. The calculation procedure consists of four stages.

At the first stage, a pressure profile is calculated for the steady flow prior to asphaltene deposition in the field. The pressure is calculated in the area of potential asphaltene deposition:

$$P_0(r) = P_{w0} + \frac{q\mu}{2\pi kh} \ln\left(\frac{r}{r_w}\right). \tag{2}$$

At the second stage, pore space is considered as a group of stream tubes with different hydraulic radius estimated on the basis of porosity. It is known that the critical diameter of particles trapped in a tube to plug it is estimated as a part of the tube hydraulic diameter.

$$D_{cr} = \alpha D_H \tag{3}$$

where α is deduced from experiments (the value = 1/3 is used for filtration).

The amount of asphaltenes precipitated in oil and trapped in pore throats is calculated as:

$$f_t = \int_{D_{cr}}^{\infty} f(D_A)\, dD_A. \tag{4}$$

At the third stage, rock porosity in the damaged area is calculated as follows:

$$m = m_0\left(1 - \frac{k_t}{k_0}\right). \tag{5}$$

Pressure drop caused by asphaltene deposition is calculated by the following equation:

$$\Delta P = \frac{\Delta P_0}{\left(1 - \frac{k_t}{k_0}\right)^2}. \tag{6}$$

The pressure after formation damage is calculated from the following equation:

$$P = P_0 - \Delta P. \tag{7}$$

At the fourth stage, the pressure drop corresponding to the skin factor is calculated:

$$P_0 - P_w = \frac{q\mu}{2\pi k_0 h}\left[\ln\left(\frac{r_b}{r_w}\right) + S\right] \tag{8}$$

where S is the skin factor.

$$\Delta P_s = \frac{q\mu S}{2\pi k_0 h} \tag{9}$$

$$\Delta P_s = P_w - P_{w0}. \tag{10}$$

Taking into account Eq. 10, the skin factor is calculated from Eq. 9.

This technique was used to tune the dynamic model in a simulator. The parameters involved in the tuning were porosity, pressure drop, and skin factor.

The novelty of this paper is that the authors for the first time estimated formation damage caused by asphaltene deposition in one of the Russian oilfield by a complex of methods including the filtration method, micro-computed tomography and dynamic modeling. Using a set of research methods makes it possible to predict formation damage.

Experiment methods and development

Laboratory apparatus

Asphaltene precipitation in oil was studied by a PVT (pressure–volume–temperature) unit via the light scattering method (1 nm sensitivity of the system), high-pressure microscopy with programmed grain size analysis (1 μm sensitivity of the system) and the gravimetric method. The scheme of the measuring system is presented in Fig. 1.

The main components of the unit were: SDS (solid detection system) PVT cell (the source and the radiation detector installed in the cell) where energy of the scattered light passing through the investigated fluid were measured (appearance of solid phase in oil was noted by a sharp decrease in energy of scattered light); HPM (high-pressure microscope) cell (consists of a cell body and two sapphire glasses between which the investigated fluid circulates) where micrographs of the fluid are recorded by a high-pressure microscope; a solid filter for organic particles (1 μm filter size) through which a specific volume of fluid sample has to be filtered to measure the weight of deposited asphaltenes; pump P1 (with volume of 500 ml) which maintain required pressure in the system; pump P2 (with volume of 10 ml)

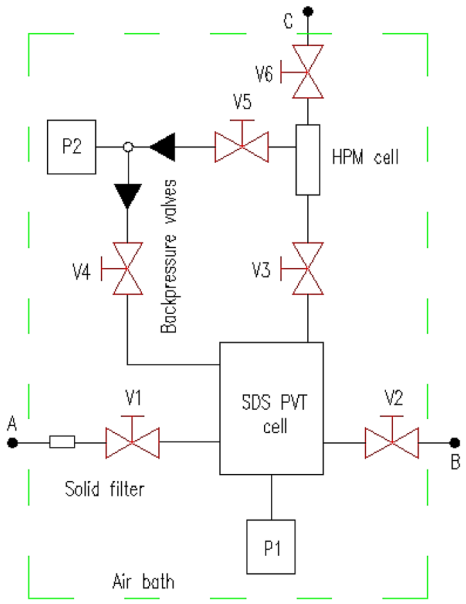

Fig. 1 Schematic diagram of the PVT unit. (P)—pump, (V)—valve, (A, B, C)—connection points of the external equipment

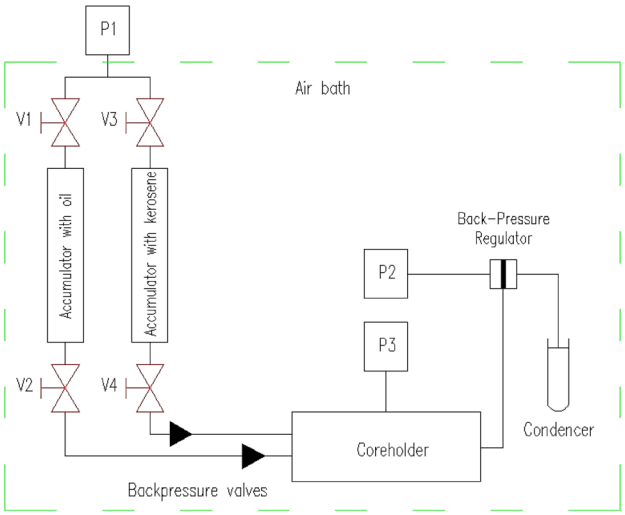

Fig. 2 Schematic diagram of the filtration equipment. (P)—pump, (V)—valve

which pumped the fluid through a closed loop of the system to achieve its homogeneity.

The required temperature of the system was maintained by an air bath (oven). Data recording (temperature, pressure, volume, micrographs, and light transmitting power) was provided on-line by a computer every 30 s. Operating temperature inside the unit can be maintained in automatic mode in temperature range from − 20 to 200 °C, and the maximum operating pressure of the unit was 69 MPa. The minimum oil volume to be examined was 30 ml, and the maximum oil volume was 60 ml.

Flow of oil, kerosene and water through a core sample were carried out by the installation which scheme is shown in Fig. 2. The main units of the installation were: oil and kerosene storage tanks with volume of 1 l each (discharge lines of the tanks face downwards to prevent displacement of hydrocarbon gas from the storage tank to the core holder in case of oil degassing), the core holder, the backpressure regulating valve (with 69 MPa operating pressure), the condenser (graduated tank enabling to measure the displaced fluid volume), the P1 and P2 pumps. Differential pressure transducers are installed at the inlet and outlet of the core holder. Confining pressure in the core holder is provided by the P3 pump. All the units are located within an air bath (oven). Operating temperature and pressure of the installation are 200 °C and 69 MPa, respectively.

Optical properties of oil were measured by a spectrophotometer which consists of a radiation source, a detector, a radiation wavelength regulator, and a measuring cuvette. Operating conditions were: ambient pressure and temperature. In the study, the cuvettes were used which are made of optical glass with a length of 50 mm.

3D models of the pore space were obtained after scanning the core by a microcomputer tomograph before and after asphaltene deposition.

Dynamic modeling of fluid flow in the model of the porous medium obtained after scanning was performed via dynamic simulator.

Oilfield overview and sample properties

The oilfield discovered in 1944 is one of the oldest field developed in the Samara region. Its target formation was brought into commercial production in 1953 and is characterized by a good dynamic connectivity with the boundary water-drive system and its high-production potential. Implemented after 20 years of production, the reservoir pressure maintenance (RPM) system has negligible impact on energy characteristics of the reservoir. Numerous old oilfields in the Samara region developed for a long time with the RPM system are distinguished by a decrease in reservoir temperature which complicates the fields' operation (oils in most Samara oilfields are characterized by a high content of wax). A minor formation was brought into production in 1953. The field under study is distinguished by poor connection with the edge aquifer; reservoir pressure is sensitive to the field operation. Therefore, the RPM system was implemented there after several years of development. Forced oil production led to a significant decrease in reservoir pressure. In a number of wells, a decrease in downhole pressure below the bubble-point pressure was obtained. Production wells are operated with low flow rates and high water cut. In the period since 1970–2017, 98 wells-operations were carried

Table 1 Properties of the reservoir oil sample

Reservoir temperature (°C)	48
Reservoir pressure (MPa)	20
Sampling depth (m)	2000
Gas/oil ratio (m^3/m^3)	45.6
Resin content (% weight)	3
Asphaltene content (% weight)	0.76
Wax content (% weight)	6
Saturates (% weight)	77.94
Aromatics (% weight)	18.3
Viscosity (mPa s)	2.1
Gravity, g/cm^3	0.828

Table 2 The main core sample properties

Length (m)	0.0814
Diameter (m)	0.0301
Porosity (%)	16.5
Pore volume (ml)	9.54

out in the oilfield to treat downhole well zones with hot oil, surfactant solutions and solvents to remove asphaltenes and wax deposits. Now, the oilfield is operated at a final stage of development with high depletion of reserves.

In this paper, reservoir oil with a density of 0.828 g/cm^3 from this field was studied which main properties are presented in Table 1. Oil was sampled from a 2000 m depth by a downhole sampler. After that, the sampler was delivered to the laboratory under maintaining the reservoir pressure and temperature, and the experiments were provided. The well is operated by an electric submersible pump with low oil rates. Over the past few years, the well has been undergoing workovers related to cleaning of flowlines from organic deposits.

High-molecular components (Saturates, Aromatics, Resins, Asphaltenes) were separated from oil by the SARA method. According to the SARA analysis, oil components are divided into four groups: Saturates (saturated hydrocarbons), aromatics (aromatic hydrocarbons), resins and asphaltenes.

In the filtration experiment, a terrigenous core was used which parameters are presented in Table 2. The core was selected from a payzone where oil was sampled from.

Measurement procedures

Visual method of study, light scattering method, and gravimetric method

Asphaltene deposition in oil were studied as follows: 40 ml of oil preheated to the reservoir temperature was transferred under the reservoir pressure from a sampler to the measuring system filled with nitrogen at the reservoir pressure and temperature. After that, nitrogen and 10 ml of oil were slowly evacuated from the top of the unit to the atmosphere. Then, circulation of oil started through the closed loop: SDS cell–HPM cell–SDS cell. Under these conditions, the system was maintained for 12 h to ensure oil homogeneity. A computer recorded the parameters of the measuring systems: Radiation power (the light scattering method), amount and size of solid particles in oil (visual analysis), and the PVT properties of oil.

Upon stabilization of these parameters, pressure was isothermally reduced from reservoir pressure to onset pressure (at the reservoir temperature) in oil with pressure depletion rate of 2.6 MPa/h. A computer recorded the experimental data. As soon as the asphaltene onset pressure was recorded (pressure of 6.8 MPa with saturation pressure of 6.5 MPa) (by visual and the light scattering methods), 10 ml of oil was pumped through a solid filter for organic particles (the gravimetric method). After that, the experiment was stopped and the filter was removed from the installation, dried to constant weight and weighed. The gain of the filter weight is equal to the weight of solid organic deposits (asphaltenes). After that, the deposits were dissolved in toluene, and their complete dissolution indicated that those were asphaltene particles with aromatic nature.

Filtration method

The filtration method had the following features: measurements of the core permeability were carried out under steady-state conditions, i.e., at low and constant flow rates of fluid (oil, kerosene, and water) through the core sample. Initially, the core was extracted with an alcohol-benzene mixture in the Soxhlet apparatus and dried to constant weight. After that, the core weight was measured as equal to 127.024 g. Then, the core was placed in a filtration unit wherein the reservoir thermobaric conditions were maintained. A tank with kerosene was connected with the core holder. The core was then saturated with kerosene at a constant temperature of 48 °C (reservoir temperature), confining pressure of 22 MPa (reservoir pressure), back-pressure of 17 MPa, and flow rate of 0.5 ml/min for five

pore volumes (until the core was fully saturated). After that, the experiment divided into five stages began. The experiment stages followed continuously one after another.

Stage 1: 3.60 pore volumes of kerosene was filtered through the core until pressure drop equal to $\Delta P = 0.079$ MPa became stable (pressure was measured by differential pressure gauges at the inlet and outlet of the core holder). This filtration stage was carried out under the following conditions: reservoir temperature of 48 °C, confining pressure of 22 MPa, backpressure of 17 MPa and kerosene flow rate of 0.5 ml/min. After that, filtration was stopped. This stage is needed to saturate the core with kerosene so that no air remains in the pore space of the core, and gas would not escape from the formation oil at the beginning of filtration, also, to measure the initial relative permeability of kerosene.

Stage 2: The tank with kerosene was disconnected (reservoir pressure and temperature were retained in the core holder), a tank with formation oil was connected to the core holder and 8.00 pore volumes of oil was filtered until pressure drop became stable ($\Delta P = 0.175$ MPa which corresponds to the pressure drop in the uninvaded formation zone) under the same thermobaric conditions as in stage 1. Then filtration was stopped.

After that, backpressure was reduced from 17 to 6.8 MPa.

Stage 3: 2.80 pore volumes of oil was filtered until pressure drop became stable ($\Delta P = 0.186$ MPa which corresponds to the pressure drop in the uninvaded formation zone). After that, filtration was stopped.

Then, backpressure was reduced from 6.8 to 5.6 MPa.

Stage 4: 17 pore volumes of oil was filtered until pressure drop became stable ($\Delta P = 0.260$ MPa which corresponds to the pressure drop in a wellbore zone). After that, filtration was stopped. The tank with oil was disconnected and the tank with kerosene was connected to the core holder.

After that, backpressure was increased from 5.6 to 17 MPa.

Stage 5: 7.00 pore volumes of kerosene were filtered until pressure drop became stable ($\Delta P = 0.089$ MPa) under the thermobaric conditions of stage 1 (backpressure of 17 MPa and reservoir temperature). After that, filtration was stopped. At all the stages, the confining pressure was equal to reservoir pressure of 22 MPa.

Then, the core was removed from the unit, dried to constant weight at temperature of 105 °C and weighed.

Stage 6: A tank with water (NaCl solution with concentration of 5 g/l, that is, the formation water model) was connected to the core holder and 3.0 pore volumes of water was filtered through a dried core until pressure drop ($\Delta P = 0.146$ MPa) was stabilized under thermobaric conditions as in stage 1. Then filtration was stopped. After that, the core was extracted with an alcohol–benzene mixture in the Soxhlet apparatus (to remove deposited asphaltenes and inorganic particles), then five pore volumes of kerosene was filtered to saturate the core (under thermobaric conditions, as in stage 1). Then, filtration was stopped and the core was dried again until a constant weight was attained (to reproduce wettability similar to the initial conditions of the filtration stage 6).

Stage 7: Again, a tank with brine was connected to the core holder. Then, 3.0 pore volumes of water was filtered through the core until pressure drop became stable ($\Delta P = 0.131$ MPa) under thermobaric conditions, as in stage 1. After that, filtration was stopped.

After each stage filtration, permeability of the core was calculated by Darcy's law (K_{ki}, K_{kd}, K_{oi}, K_{od}, K_{wi}, K_{wd}). The k, o, w subscripts mean kerosene, oil, water, respectively; i, d are the initial permeability and permeability of the damaged core, respectively. Since permeability of the core decreases, this indicates formation damage caused by asphaltene deposition.

Photocolorimetric method

Optical density of oil indirectly indicates the state of asphaltene particles in oil. After each stage of filtration, degassed oil was collected in separate tanks different for each stage. From each tank (corresponding to filtration stages 2, 3 and 4), three oil samples were collected (from the bottom, the middle and the top of each tank) and investigated by the photocolorimetric method. Three tests were averaged. The method is based on measuring attenuation of a parallel beam of light (in the visible spectrum) as it propagates through absorbing medium (oil dissolved in a diluent). Operating wavelength of the spectrophotometer is within the range of 315–1000 nm. For light oil, it is conventional to carry out experiment in a narrower range. Therefore, emission spectrum was recorded in the wavelength range of 340–610 nm.

Optical density of degassed oil was measured in cuvettes with wall thickness of 1 mm. Due to high sensitivity of the unit, it was prescribed by the technique dilution of oil with optically less dense solvent. The contribution of solvent to a decrease in optical density of oil is taken into account by parallel installing a reference cell filled with solvent to tune the unit and reset data in relation to solvent optical density. *n*-heptane which is known to precipitate asphaltenes was used as a diluent. Measurements were carried out at ambient temperature (25 °C) and pressure. For all oil samples (after each filtration stage), wavelength of 340 nm was chosen as the main wavelength in the ultraviolet spectral range.

The measurement principle was based on the Bouguer–Lambert–Beer law and asphaltenes as coloring particles in oil.

The Bouguer–Lambert–Beer law is expressed by the following equation:

$$I(h) = I_0 10^{-hC\varepsilon} \tag{11}$$

where $I(h)$ is the intensity of light passed through the layer of the solution with thickness h, I_0 is the intensity of light

before the solution, ε is the absorption coefficient which is constant for the coloring particles, and C is the solution concentration.

$$\lg \frac{I_0}{I(h)} = hC\varepsilon = D \tag{12}$$

where D is optical density of the solution, a constant value for each solution.

For two solutions of different concentrations, Eq. 12 takes the following form:

$$\frac{D_1}{D_2} = \frac{C_1}{C_2}. \tag{13}$$

For all tests, the same oil concentration in a diluent was taken so that the concentration of solution could be recalculated into the concentration of asphaltenes in oil. Thus, once the concentration of asphaltenes in original oil is known, their concentration after deposition in a core can be calculated.

Microcomputed tomography

An X-ray tomography system allows exploring internal structure of an object without its preliminary preparation or destruction. This method was proposed in 1972 by H. Hounsfield and A. Cormack. The method to study rocks is based on the difference in rock density, pores and saturating fluids. X-ray radiation passes through an object, loses its power in proportion to the rock density and is recorded by a radiation receiver generating grayscale images of the object. During scanning, the object rotates around its axis (45 min for 360° scanning). Image brightness corresponds to the degree of X-ray absorption. After that, the resulting images are reconstructed into cross-sections which serve as a 3D model constructed for the sample. The model represents distribution of sample density in the volume which enables calculating characteristics of the pore space.

An extracted and dried core (before stage 1 of filtration) was studied by the microcomputed tomography. After asphaltene deposition in the core (after stage 5 of filtration), the dried core was also examined. Two models of the porous medium were reconstructed, and the values of effective porosity and pore size distribution before and after asphaltene deposition were obtained.

Analysis of experiment results

Even though the ratio of resin to asphaltenes is greater than 1.25 (equal to 3.95), the colloidal instability index is 3.69 which indicates that initial oil is disposed to precipitate asphaltenes when thermobaric conditions change.

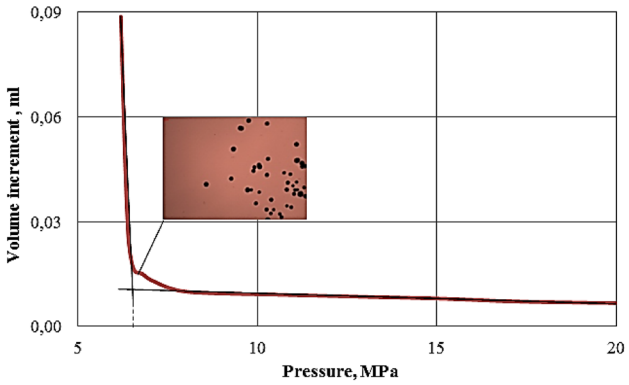

Fig. 3 Volume increment of oil versus pressure at reservoir temperature (48 °C)

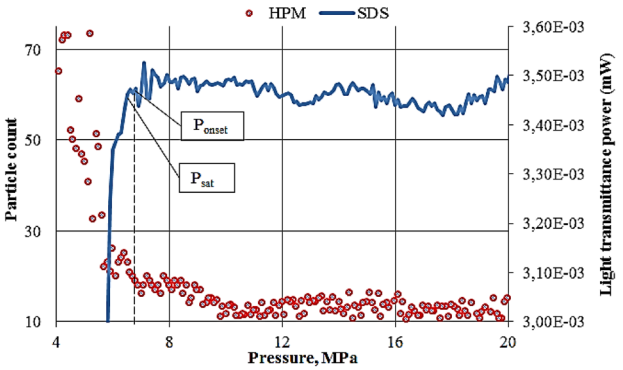

Fig. 4 Light transmittance power and particle count versus pressure

Visual method of investigation, light scattering method, gravimetric method

The bubble-point pressure was measured with the PVT unit by measuring changes in pressure and volume (Fig. 3).

The graph shows that the bubble-point pressure is 6.5 MPa. This is confirmed by a micrograph recorded with a high-pressure microscope at a pressure of 6.5 MPa and temperature of 48 °C where the first bubbles of gas can be observed (Fig. 3).

Two independent methods (high-pressure microscopy and the light scattering method) show that asphaltene particles begin to aggregate at pressure of 6.8 MPa and this process reaches a maximum at the bubble-point pressure (6.5 MPa) (Fig. 4). Figure 5 shows the micrographs of oil before and after the beginning of asphaltene precipitation at isothermal pressure depletion.

Just above the bubble-point pressure (6.8 MPa) the micrographs show that the first solid particles (asphaltenes) with average diameter of 4.4 μm appear.

Figure 6 shows samples of asphaltene deposits after oil was pumped through a solid filter for organic particles.

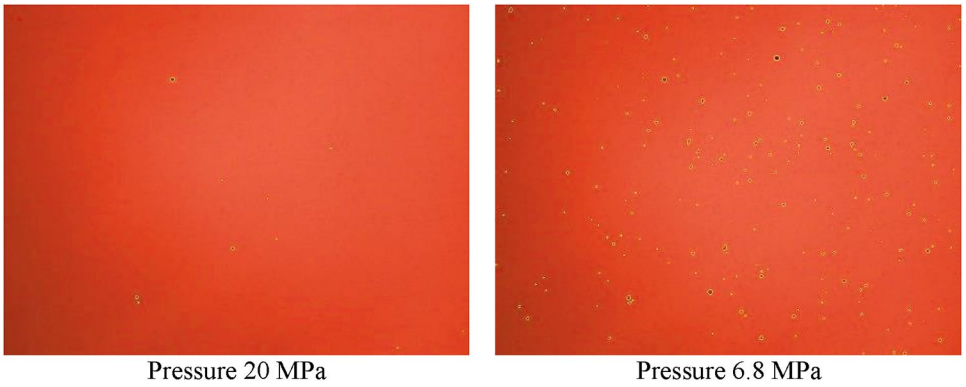

Fig. 5 Micrographs of oil sample at isothermal (48 °C) pressure depletion (magnification of 100)

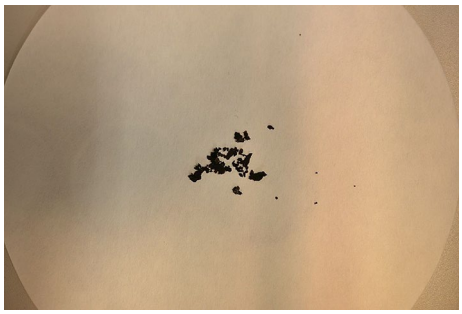

Fig. 6 Asphaltene sample after pumping of oil through organic solid filter

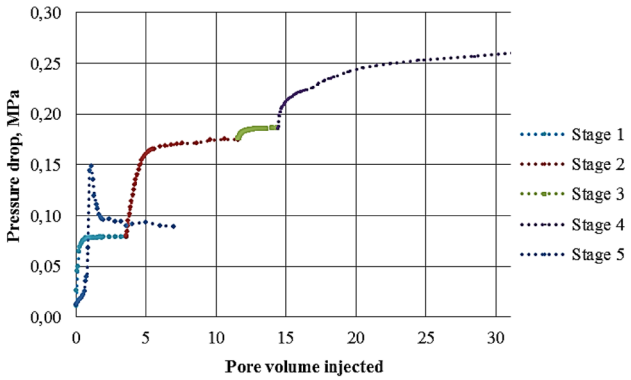

Fig. 7 Pressure drop versus pore volume injected at different back pressures

Deposits were dried and further were not specially prepared in any way and are presented in the picture in the raw. The sizes of separate asphaltene aggregates can reach from 1 to 3 mm.

Filtration method

Permeability (damage rock permeability of oil) caused by formation damage as well as initial permeability were calculated according to Darcy's law. Permeability decreases as backpressure decreases (increase in pressure drop). Partial liberation of gas from oil in the core causes the asphaltene deposition which accelerates with increasing shear rate (pressure drop) causing the trapping of asphaltene particles in the core. A similar mechanism can be observed in reservoirs with low permeability in the near-wellbore area.

At filtration stage 1 (Fig. 7), pressure gradient rapidly becomes stable after pumping several pore volumes of kerosene through the core. This indicates that the fluid does not interact with the pore space surface. At filtration stages of 2 and 3, stabilization of the pressure gradient takes a longer time. This indicates that asphaltene deposition in the porous medium begins slightly. Thus, at filtration stage 3, there is a slight decrease in relative permeability of oil. During the experiment, backpressure was 6.8 MPa, i.e., pressure at the core outlet was equal to the asphaltene onset pressure. An insignificant amount of aggregated asphaltene particles with sizes comparable to the size of pore throats can be assumed, as well as insufficient time for their aggregation and deposition.

Figure 7 shows that at filtration stage 4, pressure gradient did not become stable during the experiment. That is, pressure drop along the core gradually increased throughout the entire filtration stage. This may be due to the fact that asphaltenes were continuously deposited in the pore space of the core. A larger pressure gradient led to accelerated precipitation and aggregation of asphaltenes in oil. The number of particles with dimensions comparable to pore sizes became significantly greater than at stage 3. As a result, relative permeability of oil after stage 4 considerably reduced.

Thus, five experiments have been carried out in different conditions (backpressures, phases: at a stage 1—kerosene, at stages 2, 3 and 4—reservoir oil, at a stage 5—kerosene was filtered). The pressure drop increase not dramatically if to compare stages 2, 3 and 4 (oil filtration). If to compare stages 1 and 2, then the pressure drop increases considerably since properties of fluids are very different. Aggregation of asphaltenes takes some prolonged period comparable to the experiment duration. Respectively, pressure drop gradually increases over time as a result

of asphaltene aggregation, their trapping into the porous medium, deposition and clogging of pore throats.

In this paper, authors have tried to reduce quantity of the factors influencing asphaltene deposition to study effect of pressure upon this process in more detail. A major factor which causes asphaltene precipitation is pressure decrease lower onset pressure which is slightly higher bubble-point pressure. Gas begins to liberate from oil at a bubble-point pressure, so that thermodynamic equilibrium in oil is disturbed, it's dissolving ability in relation to asphaltenes considerably decreases, the maximum asphaltene precipitation rate is observed at this pressure. Further migration of asphaltene particles in the porous medium is influenced by four major factors, such as diffusion, adsorption, sedimentation and fluid forces.

The core permeability before and after asphaltene deposition was calculated using Darcy's law (Permeability is calculated based upon the measured pressure drop along the core through Darcy's law):

$$K = \frac{\mu LQ}{A\Delta P} \tag{14}$$

where K is permeability of the core (initial permeability), m^2; μ is viscosity of fluid (fluid viscosity), Pa s; L is the core length (effective core length), m; Q is total volumetric flow rate through the core, m^3/s; A is cross-sectional area of the core sample, m^2; ΔP is pressure drop along the length of the core sample for a set flow (pressure drop along the length L), Pa.

The permeability damage factor (K_{DF}) due to asphaltene deposition is calculated by the following equation:

$$K_{DF} = \left(1 - \frac{K_d}{K_i}\right) \times 100 \tag{15}$$

where K_d is permeability of the damaged core, and K_i is the initial permeability.

In these experiments, constant flow rate was maintained during each filtration stage. If we assume oil viscosity during filtration for a constant value, then the ratio in the right side of Eq. 15 takes the following form:

$$\frac{K_d}{K_i} = \frac{\Delta P_i}{\Delta P_d}. \tag{16}$$

Weight of the dried core before asphaltene deposition was 127.421 g. The difference in weight of the dried core before and after oil filtration corresponds to the weight of deposited asphaltenes in the pore space which was 0.397 g (Table 3).

In conditions of forced production in the field, pressure gradient in the near-wellbore area can reach large values, and the drawdown cone will extend further away from the well with time. Therefore, during oilfield development,

Table 3 Results of filtration experiments

Filtration stage	Pressure drop (MPa)	Back pressure (MPa)	Pore volume injected	Initial oil permeability (K_{oi}) (mD)	Damage oil permeability (K_{od}) (mD)	Initial kerosene permeability (K_{ki}) (mD)	Damage kerosene permeability (K_{kd}) (mD)	Initial water permeability (K_{wi}) (mD)	Damage water permeability (K_{wd}) (mD)	Permeability damage factor (K_{DF}) (%)
1	0.079	17	3.60	–	–	25.34	–	–	–	–
2	0.175	17	8.00	11.44	–	–	–	–	–	–
3	0.186	6.8	2.80	–	10.76	–	–	–	–	5.91
4	0.260	5.6	17.0	–	7.70	–	–	–	–	32.69
5	0.089	5.6	7.00	–	–	–	22.49	–	–	11.24
6	0.146	17	3.00	–	–	–	–	–	6.53	–
7	0.131	17	3.00	–	–	–	–	7.28	–	10.27

Applied flow rate of oil = 0.5 ml/min

the area affected by asphaltene deposition may also extend deep into a formation.

Photocolorimetric method

The experiment results showed that optical density of oil (Fig. 8) decreases after each subsequent filtration stage because asphaltenes are deposited on the surface of the pore space and their concentration in oil at outlet from the core is reduced. It can be assumed that relative change in optical density will characterize the same relative decrease in the amount of asphaltenes in oil in accordance with the Bouguer–Lambert–Beer law. Optical density of the initial oil corresponds to asphaltene concentration of 0.76% by weight. In accordance with Eq. 13, concentrations of asphaltenes in oil after filtration stages of 2, 3 and 4 are 0.69%, 0.59% and 0.36%, respectively. Degassed oil in the core (filtration stage 4) has the lowest optical density.

To calculate the amount of asphaltenes deposited in the core, the following equations were used.

Duration of contacting of oil with the core:

$$t = \frac{\pi m D^2 L}{4Q} n \tag{17}$$

where m is porosity of the core, fraction, D is diameter of the core, cm, L is length of the core, cm, Q is oil flow rate, cm^3/min, n is the number of pore volumes of injected oil.

The weight of asphaltenes deposited in the pore space is a function of time and can be calculated by the following equation:

$$m_a(t) = \frac{1}{4}\pi m D^2 L \rho \left(\omega_i - \int_0^{t_{end}} \omega(t)\,dt \right) \tag{18}$$

where ρ is density of oil at the inlet of the core, g/cm^3.

The value of $\int_0^{t_{end}} \omega(t)dt$ was found from the Bouguer–Lambert–Beer equation (for filtration stage 4) equal to 0.36%. As a result of oil flow through a core sample with pressure drop of 2.6 MPa, the concentration of asphaltenes in oil decreased in 5.7 h from 0.59% (at the beginning of filtration stage 4) to 0.36% (at the end of filtration stage 4).

Thus, the calculated weight of deposited asphaltenes after filtration stage 4 was 0.419 g which was slightly higher than the measured value (0.397 g). Thus, direct measurement (measurement of weight) is more reliable, while accuracy of the calculated value is limited by measurement accuracy for the parameters included in Eq. 18. The highest error occurred when measuring concentration of asphaltenes before and after deposition in the core.

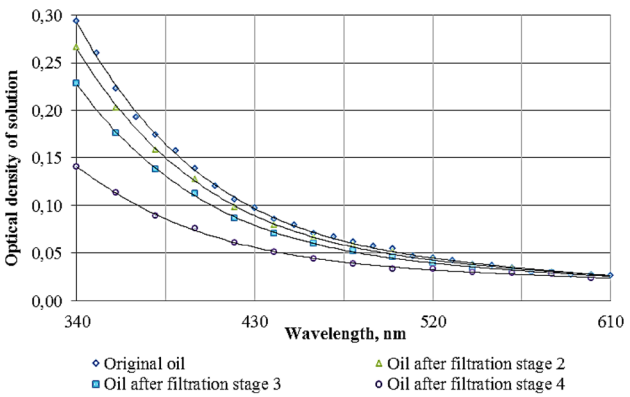

Fig. 8 Optical density of solution versus wavelength

Microcomputed tomography

Three-dimensional models of the pore space of the investigated core before and after oil filtration were constructed by an X-ray computer micro-tomograph. A 3-D model of the rock matrix (core) obtained before oil filtration is shown in Fig. 9. The results of comparison of the models indicate a significant decrease in porosity due to asphaltenes adsorbed on the surface of rock grains. The analysis results for changes in porous space show that porosity decreased from 16.5 to 13.2% after asphaltene deposition. Figure 10 shows the size distribution of pore throats within the range of pore diameters from 1 to 18 μm.

Plugging of pores is related to small-sized pores (with diameters smaller than 12 μm) comparable in size with asphaltene particles formed in oil. Asphaltene deposition affected only the pores with diameter below 12 μm. Pores with sizes comparable with asphaltene particles were plugged by them. In those pores, which sizes slightly exceeded particle sizes, adsorption of asphaltenes occurred. The rest of the pore sizes were not included in the considered range. It can be assumed that mechanical trapping of asphaltenes in pore throats is the predominant one. The experiment results showed that large-sized pores were not involved in asphaltene deposition which was confirmed by a number of researchers (Shedid and Zekri 2006; Papadimitriou et al. 2007).

Figure 10 shows that asphaltene deposition in the core resulted in plugging 54% of the pore space in the range of pore diameters from 1 to 18 μm. Asphaltene deposition mostly affected pore throats within the range of diameters from 1 to 6 μm comparable with the size of asphaltene particles.

Simulation of asphaltene deposition in porous medium

In the dynamic model, a porous medium is represented by two continuously permeable and impermeable pathways.

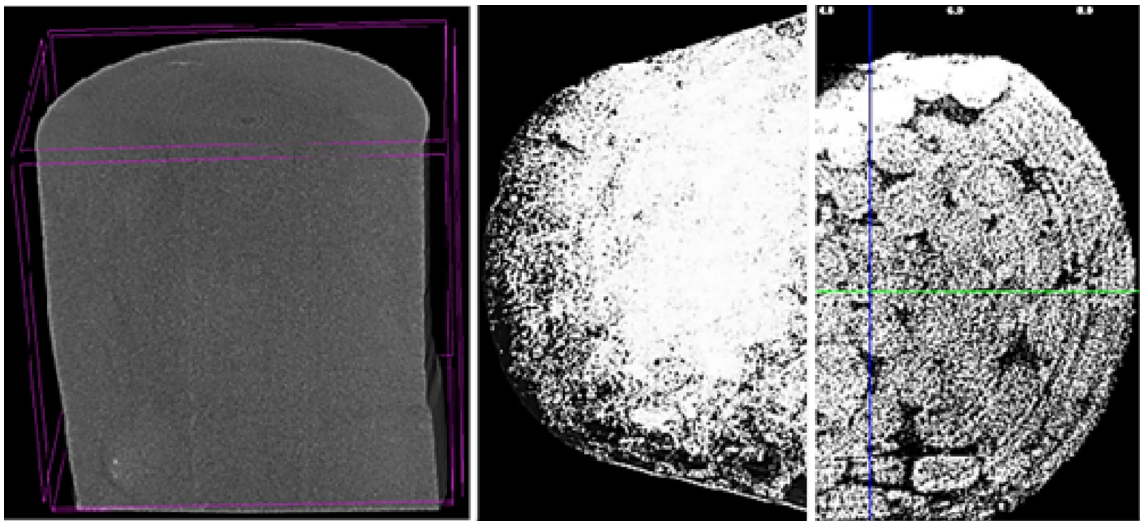

Fig. 9 3-D model of core sample

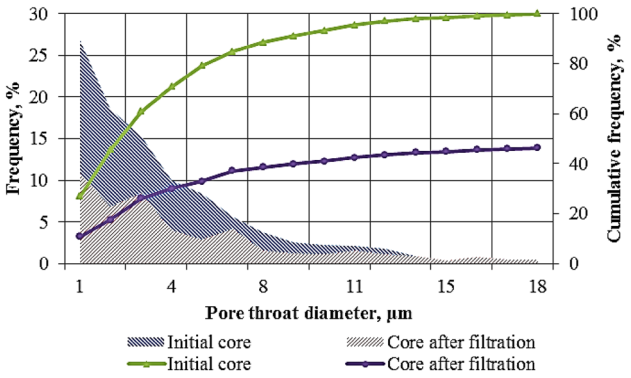

Fig. 10 Pore throat diameter distribution before and after filtration

Asphaltene deposition causes reduction in hydraulic diameter of pores, correspondingly, porosity and permeability. A dynamic model (fluid flow in a porous medium) can be constructed by specifying a full-porosity model. A porosity model includes both a generalization of the Navier–Stokes equations and of Darcy's law. In those areas of the model where geometry of pore channels is too complicated, it is possible to set the resistance to flow coefficients. In this case, the model contains a diffusion term.

In the model, generalized Darcy's law was used which has the following form:

$$-\frac{\partial p}{\partial x_i} = \frac{\mu}{k} U_i + k_{\text{loss}} \frac{\rho}{2} U_i^2. \tag{19}$$

Loss coefficient can be given as:

$$k_{\text{loss}} = -\frac{2\Delta P A^2}{\rho L Q^2}. \tag{20}$$

In accordance with the abovementioned, two dynamic models were constructed based on data obtained from core scanning and filtration experiments before and after asphaltene deposition. Porous domains were created. The results of tuning of the dynamic models to the parameters observed in filtration experiments in accordance with the procedure proposed by Leontaritis are shown in Figs. 11 and 12.

Figures 11 and 12 show the velocity fields in three sections of a core sample for two dynamic models, as well as stream tubes. The direction of fluid flow coincides with the *Y*-axis direction. It can be seen from the figures that the maximum flow velocities of the fluid for the initial sample have larger values with respect to the damaged sample.

After asphaltene deposition, the number of areas with higher flow rates increased, however, they decreased in size, also the flow velocity decreased, and the areas with zero flow velocity appeared. The simulation results showed that asphaltene deposition in a porous medium was irregular, thus, the main filtration channels were redistributed.

Optimal methods to prevent asphaltene deposition in the near-wellbore area

Management of the well-operating conditions and the use of inhibitors (Hirschberg et al. 1982) are the most technological methods aimed to prevent or slow down this complication. The first method is aimed at lowering drawdown information which prevents the liberation of gas from oil in the near-wellbore area. Many wells in the field operated by ESP are equipped with frequency controlling apparatus which allow regulating the well flow rate without ESP replacement. Well flow rate does not have to be regulated all the time. It is necessary to decrease the well flow rate once by a certain

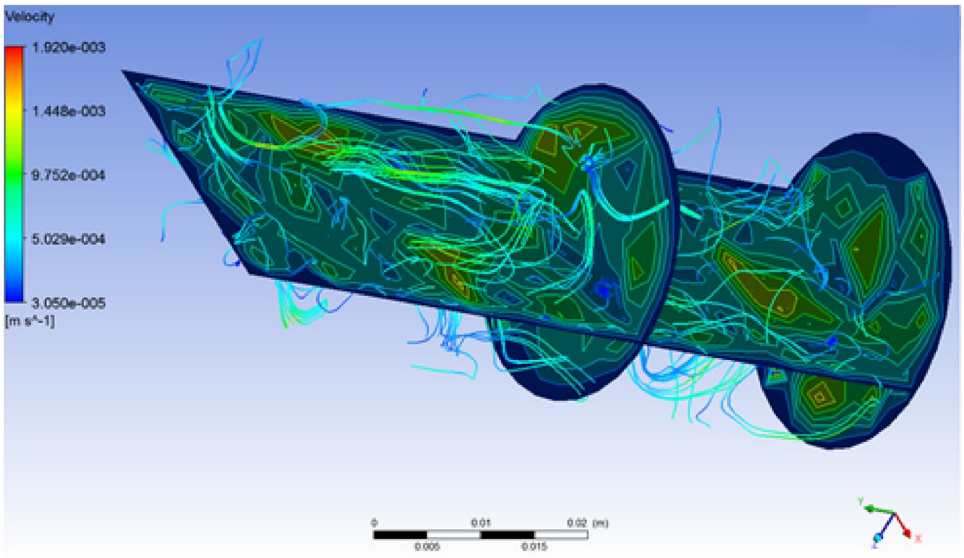

Fig. 11 Profile of flow velocities across pore throats before asphaltene deposition

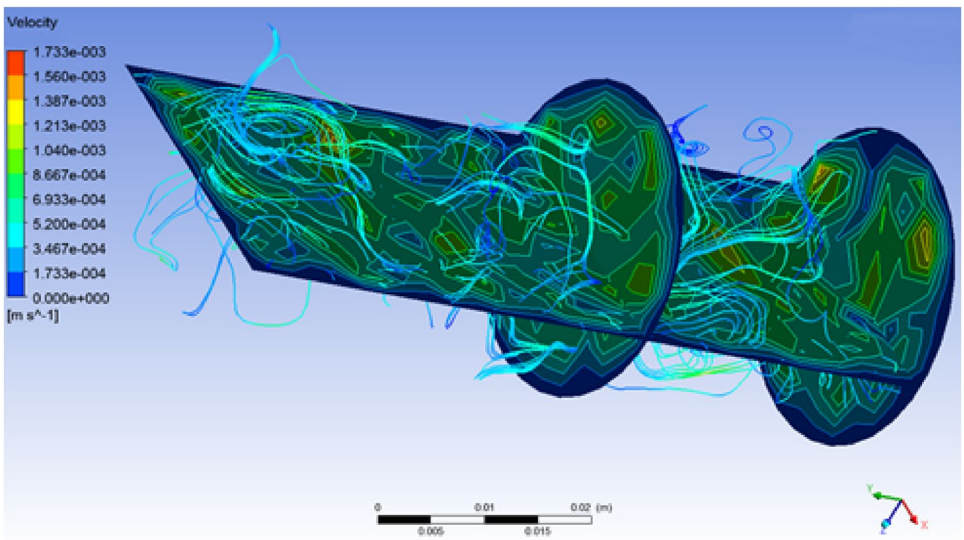

Fig. 12 Profile of flow velocities across pore throats after asphaltene deposition

value depending on current downhole pressure until the next reduction of the downhole pressure.

The second method is chemical. The authors of the paper (Struchkov and Rogatchev 2014) developed an inhibitor absorbed on the surface of asphaltene particles that prevents their aggregation. The proposed technology consists in injecting hydrocarbon solution of the inhibitor into a pay zone. The inhibitor will be desorbed from the reservoir and in some concentration flowed with oil into the well during production. Thus, asphaltenes precipitation and deposition will be decreased. And during shutdown, some concentration of the inhibitor will be presented in oil. Before shutdown, it is necessary to clean up the well with a hydrocarbon solution with inhibitor in some concentration. So that a film of the inhibitor will be formed on the tubing surface thus reducing the adhesive ability of asphaltenes and plugging of the well will be slowed down. Detailed technology parameters can be presented only after additional laboratory studies.

A technological method can be combined with the chemical one to reach the highest efficiency to manage the organic scales.

Conclusions

- The visual method allows measuring sizes of solid particles in oil when thermobaric conditions change as well as estimating the probability of their deposition in the rock pore space via microcomputed tomography. The gravimetric and filtration methods allow quantitative assessment of asphaltene deposition and formation damage.

- Microcomputed tomography serves as a reliable non-destructive tool to study porous medium before and after changing its properties. The results of microcomputed tomography can be further successfully used to construct a dynamic model that allows visualizing the processes within the rock and predicting possible complications.
- The research results have shown that spectrophotometry can be a good tool to monitor development of oilfields to establish the causes and predict formation damage.
- The results of complex studies have shown that small-sized pores comparable to asphaltene particles in size are more prone to plugging than large-sized pores.
- The experiments have shown that backpressure decrease leads to a pressure drop increase and increases the amount of asphaltene deposits in porous medium. Thus, maintaining a required downhole pressure can significantly reduce formation damage caused by asphaltene deposition.
- The most optimal methods to reduce formation damage are the control of well-operating conditions and chemical methods.

Acknowledgements We acknowledge Dr. A. V. Petukhov for his assistance during the experiments. Finally, we would like to thank Saint-Petersburg Mining University (Saint Petersburg, Russia) for providing laboratory equipment support and samples for this research.

References

Ali MA, Islam MR (1998) The effect of asphaltene precipitation on carbonate-rock permeability: an experimental and numerical approach. SPE Prod Facil 13(03):178–183

Bunger JW, Li NC (1981) Chemistry of asphaltenes. American Chemical Society

Burke NE, Hobbs RE, Kashou SF (1990) Measurement and modeling of asphaltene precipitation. J Pet Technol 42:1440–1446

de Pedroza TM, Calderon G, Rico A (1996) Impact of asphaltene presence in some rock properties. SPE Adv Technol Ser 4(01):185–191

Gruesbeck C, Collins RE (1982) Entrainment and deposition of fine particles in porous media. SPE J 22(6):847–856

Hirschberg A, Jong L, Schipper B, Meyers J (1982) Influence of temperature and pressure on asphaltene flocculation, paper 11202. SPE annual technical meeting and exhibition, New Orleans, LA, 26–29 September 1982

Hirschberg A, DeJong LNJ, Schipper BA, Meijer JG (1984) Influence of temperature and pressure on asphaltene flocculation. Soc Petrol Eng J 24(03):283–293

Khalil CN, Rocha NO, Silva EB (1997) Detection of formation damage associated to paraffin in reservoirs of the Reconcavo Baiano, Brazil. Society of Petroleum Engineers, Houston

Kokal S, Al-Kaabi A (2010) Enhanced oil recovery: challenges & opportunities. World Petroleum Council: Official Publication, Istanbul, p 64

Leontaritis KJ (1989) Asphaltene deposition: a comprehensive description of problem manifestations and modeling approaches. Society of Petroleum Engineers, Ahmedabad. https://doi.org/10.2118/18892-MS

Minssieux L (1997) Paper SPE 37250 presented at the SPE international symposium on oil field chemistry held in Houston, TX, pp 401–419

Mozaffari S, Tchoukov P, Atias J, Czarnecki J, Nazemifard N (2015) Effect of asphaltene aggregation on rheological properties of diluted athabasca bitumen. Energy Fuels 29(9):5595–5599

Mozaffari S, Tchoukov P, Mozaffari A, Atias J, Czarnecki J, Nazemifard N (2017) Capillary driven flow in nanochannels—application to heavy oil rheology studies. Colloids Surf A 513:178–187

Nellensteyn FJ (1924) The constitution of asphalt. J Inst Pet Technol 10:311

Novosad Z, Costain TG (1990) Experimental and modeling studies of asphaltene equilibria for a reservoir under CO_2 injection. In: SPE Annual Technical Conference and Exhibition. Society of Petroleum Engineers, pp 71–76

Papadimitriou NI, Romanos GE, Charalambopoulou GC, Kainourgiakis ME, Katsaros FK, Stubos AK (2007) Experimental investigation of asphaltene deposition mechanism during oil flow in core samples. J Pet Sci Eng 57(3):281–293

Sahimi M, Mehrabi AR, Mirzaee N, Rassamdana H (2000) The effect of asphaltene precipitation on flow behavior and production of a fractured carbonate oil reservoir during gas injection. Transp Porous Media 41(3):325–347

Sharma MM, Yen TF, Chilingarian GY, Donaldson EC (1985) Some chemical and physical problems in enhanced oil recovery operations, in enhanced oil recovery I—fundamentals and analysis. In: Donaldson EC, Chiligarian GY, Yen TF (eds) Developments in petroleum science, vol 17A. Elsevier, Amsterdam, pp. 223–249

Shedid SA (2001) Influences of asphaltene deposition on rock/fluid properties of low permeability carbonate reservoirs. In: SPE Middle East Oil Show. Society of Petroleum Engineers, pp 115–121

Shedid SA, Zekri AY (2006) Formation damage caused by simultaneous sulfur and asphaltene deposition. SPE Prod Oper 21(01):58–64

Speight JG, Long RB, Trowbridge TD (1984) Factors influencing the separation of asphaltenes from heavy petroleum feedstocks. Fuel 63(5):616–620

Struchkov IA, Rogatchev MK (2014) An impact analysis of a non-ionic surfactant on the organics state in an oil sample when modelling downhole conditions. Jelektronnyj nauchnyj zhurnal Neftegazovoe delo 5:104–118

Struchkov IA, Hamitov IG, Roshhin PV, Manasjan AJ (2016) Physical and chemical prevention methods of organic solid formation during waxy oil production. Neftepromyslovoe delo 4:48–52

Volkov VA, Prohorov PJe, Turapin AN, Afanasiev SV (2017) Cycle injection of carbon dioxide to production wells for stimulation. Theory and practice of application of enhanced oil recovery methods, pp 31–33